Characterization of Tigurilysin, a Novel Human CD59-Specific Cholesterol-Dependent Cytolysin, Reveals a Role for Host Specificity in Augmenting Toxin Activity

Ifrah Shahi[a], Sophia A. Dongas[a], Juliana K. Ilmain[b], Victor J. Torres[b], Adam J. Ratner[a,b#]

[a]New York University Grossman School of Medicine, Department of Pediatrics, New York, NY
[b]New York University Grossman School of Medicine, Department of Microbiology, New York, NY

Running Title: Host Restriction and Toxin Activity

[#]Address correspondence to Adam J. Ratner, Adam.Ratner@nyulangone.org

ABSTRACT

Cholesterol dependent cytolysins (CDCs) are a large family of pore forming toxins, produced by numerous gram-positive pathogens. CDCs depend on host membrane cholesterol for pore formation; some CDCs also require surface associated human CD59 (hCD59) for binding, conferring specificity for human cells. We purified a recombinant version of a putative CDC encoded in the genome of *Streptococcus oralis subsp. tigurinus*, tigurilysin (TGY), and used CRISPR/Cas9 to construct hCD59 knockout (KO) HeLa and JEG-3 cell lines. Cell viability assays with TGY on WT and hCD59 KO cells showed that TGY is a hCD59-dependent CDC. Two variants of TGY exist among *S. oralis subsp. tigurinus* genomes, only one of which is functional. We discovered that a single amino acid change between these two TGY variants determines its activity. Flow cytometry and oligomerization western blots revealed that the single amino acid difference between the two TGY isoforms disrupts host cell binding and oligomerization. Furthermore, experiments with hCD59 KO cells and cholesterol depleted cells demonstrated that TGY is fully dependent on both hCD59 and cholesterol for activity, unlike other known hCD59-dependent CDCs. Using full-length CDCs and toxin constructs differing only in the binding domain, we determined that having hCD59-dependence leads to increased lysis efficiency, conferring a potential advantage to organisms producing hCD59-dependent CDCs.

IMPORTANCE

Cholesterol dependent cytolysins (CDCs) are produced by a variety of disease-causing bacteria, and may play a significant role in pathogenesis. Understanding CDC mechanisms of action provides useful information for developing anti-virulence strategies against bacteria that utilize CDCs and other pore-forming toxins in pathogenesis. This study describes for the first time a novel human-specific CDC with an atypical pore forming mechanism compared to known CDCs. In addition, this study demonstrates that human-specificity potentially confers increased lytic efficiency to CDCs. These data provide a possible explanation for the selective advantage of developing hCD59-dependency in CDCs and the consequent host restriction.

49 **INTRODUCTION**

50

51 Pore forming toxins (PFTs) are produced by many pathogenic bacteria and form a diverse class
52 of bacterial protein toxins (1). PFTs likely contribute to bacterial pathogenesis in several ways,
53 including enhancement of colonization (2-4), release of host cell nutrients (5), hijacking of host
54 cell pathways (6, 7), and intracellular delivery of other virulence factors (8, 9). PFTs function by
55 perforating cell surface membranes, often leading to osmotic lysis, or triggering other
56 downstream effects, such as pro-inflammatory cell signaling cascades, membrane repair, or
57 programmed cell death (10).

58

59 Cholesterol dependent cytolysins (CDCs) are a family of PFTs produced by many gram-positive
60 bacteria (10, 11), as well as some gram-negative bacteria (12). CDCs are characterized by large
61 pores and by a dependency on host membrane cholesterol (11, 13, 14). For most CDCs, the
62 presence of cholesterol in eukaryotic cell plasma membranes is sufficient for targeting and
63 lysing a cell (11). A subset of CDCs additionally requires human CD59 (hCD59), a cell surface
64 molecule, for binding to host membranes.

65

66 CDC protein structures include four domains (15, 16). During pore formation, Domain 4 binds to
67 the target cell membrane, anchoring the CDC to the cell surface. For most CDCs, this entails
68 binding to host cell membrane cholesterol via a threonine-leucine pair conserved within the
69 Cholesterol Recognition Motif (CRM), followed by insertion of several other structural loops
70 including a conserved 11-amino acid sequence (undecapeptide [UDP]), providing anchorage
71 and stability. For hCD59-dependent CDCs, the toxin first binds to hCD59 via a conserved
72 sequence in Domain 4, before further being stabilized by cholesterol binding (16-18). Once a
73 CDC is anchored to the host cell surface, >30 units oligomerize to form a beta-barrel pore (19-
74 21). To date, four hCD59-dependent CDCs have been characterized: intermedilysin (ILY)
75 produced by *Streptococcus intermedius*, lectinolysin (LLY) produced by *Streptococcus mitis*,
76 vaginolysin (VLY) produced by *Gardnerella vaginalis*, and most recently, discoidinolysin (DLY)
77 produced by *Streptococcus mitis* (17, 22-24). Since there are few established hCD59-dependent

78 CDCs, it is difficult to form a comprehensive overview of the evolution of hCD59-dependency
79 and how that contributes to virulence for the bacteria producing such CDCs.
80
81 *Streptococcus oralis subsp. tigurinus* is a commensal bacterium found in the human oral
82 microbiome that has been implicated in invasive infections such as infective endocarditis,
83 spondylodiscitis, and meningitis (25-28). It is an α-hemolytic, non-motile, and non-spore-
84 forming bacterium. The *Streptococcus oralis subsp. tigurinus* genome includes an open reading
85 frame with sequence similarity to other hCD59-dependent CDC genomes (17, 18). Using a
86 recombinant protein, we characterized this novel hCD59-dependent CDC, tigurilysin (TGY). Of
87 the two TGY alleles present in the NCBI database, one encodes a protein that is inactive at
88 physiological concentrations, and we identified a single amino acid change in Domain 4
89 responsible for its activity. Furthermore, we delved into the question of hCD59-dependency
90 and showed that while targeting cells with hCD59 restricts such CDCs to only one species, it also
91 increases their lytic efficiency on epithelial cells by several orders of magnitude.
92
93 **RESULTS**
94
95 **There are two variants of the *Streptococcus oralis subsp. tigurinus* CDC gene**
96
97 Whole genome sequencing of three *Streptococcus oralis subsp. tigurinus* strains has revealed
98 that some, but not all, strains have an open reading frame encoding a protein with similarity to
99 previously characterized CDCs (29). We compared the amino acid sequences of *Streptococcus*
100 *oralis subsp. tigurinus* CDC (tigurilysin [TGY]) from two strains: AZ_3a and AZ_14. Five amino
101 acid differences were found between the mature predicted amino acid sequences of the two
102 variants (**Fig 1A**). We also compared TGY with amino acid sequences from other CDCs. Previous
103 studies with ILY have revealed that the toxin binds to hCD59 via residues separate from those of
104 the cholesterol-recognizing motifs (17, 30). Comparison among CDC amino acid sequences has
105 shown hCD59-binding residues to be conserved among hCD59-binding CDCs, and they are also
106 found in the TGY amino acid sequence. Furthermore, the UDP of hCD59-binding CDCs harbors a

107 proline in the 9th position instead of a tryptophan (18); this proline is also seen in the TGY amino
108 acid sequence. Based on these observations, we predicted that TGY was likely a hCD59-
109 dependent toxin (**Fig 1B**).
110
111 Recombinant His-tagged versions of TGY based on the sequences from both strains were
112 created, expressed in *Escherichia coli*, and purified. In order to assess the role of hCD59 in host
113 cell susceptibility to TGY, we utilized HeLa cells, a human cell line that expresses hCD59 (**Fig S1**).
114 We used cells that were transduced with CRISPR-Cas9 single guide RNA targeting the hCD59
115 gene (HeLa hCD59 Knockout [KO]) and HeLa control cells that have been transduced with a non-
116 targeting sgRNA (HeLa NT). We have previously used these cell lines to successfully examine ILY
117 activity and hCD59-dependency (31). The two recombinant TGY variants were tested for lysis on
118 the HeLa NT cells and HeLa hCD59 KO cells, and IC_{50} values (i.e. concentration required for 50%
119 lysis of HeLa cells) were calculated. AZ_14 TGY (TGY^{14}) lysed HeLa cells in a hCD59-dependent
120 manner (IC_{50}: 460 ng/ml), albeit at concentrations higher than those needed for lysis by ILY
121 (IC_{50}: 30 ng/ml). In contrast, the AZ_3a TGY (TGY^{3a}) did not induce lysis at the concentrations
122 tested, appearing to be inactive (**Fig 1C and 1D**). When TGY^{3a} was further tested on HeLa cells
123 at supraphysiological concentrations, it was found to cause lysis in a hCD59-dependent manner,
124 indicating that the toxin is functional but inefficient, requiring high dosages for functionality
125 (IC_{50}: 261 μg/ml) (**Fig 1E**). To confirm that this hCD59-dependent lysis is not specific to HeLa
126 cells only, both TGY variants were also tested for lysis on JEG-3 cells (a human choriocarcinoma
127 cell line) with and without hCD59 expression, with results similar to those on HeLa cells: TGY^{14}
128 lysed the cells in a hCD59-dependent manner, while TGY^{3a} remained inactive at the
129 concentrations tested (**Fig S2**).
130
131 **TGY residue at position 454 is important for lytic efficiency**
132

133 To understand the cause of TGY^{3a} inefficiency, we turned our attention to the amino acid
134 sequence differences between the two TGY variants. Of the five single amino acid differences,
135 two are in Domain 4: residue 454 and residue 505 (**Fig 1A**). Residue 505 incorporates an
136 isoleucine in TGY^{3a} and a leucine in TGY^{14}. Based on amino acid sequences of other CDCs, this
137 residue position seems to be permissible for both amino acids – some CDCs have an isoleucine
138 while others have a leucine, without any correlation to the species specificity of the CDC.
139 Conversely, residue 454 is part of the short hydrophobic loop known as Loop 2 (L2), one of the
140 three conserved CDC loops that insert into the host membrane in a cholesterol-dependent
141 manner (32, 33). In most CDCs, the corresponding amino acid in L2 is an alanine; however, non-
142 functional TGY^{3a} harbors a glutamic acid (E) at this position, while the functional TGY^{14} has a
143 glycine (G). Additionally, both TGY variants have an isoleucine (I) instead of a leucine (L) at
144 position 544, which is part of the conserved CRM threonine-leucine pair.
145
146 Using site-directed mutagenesis, we made three amino acid substitutions in TGY^{3a}, resulting in
147 TGY^{3a_E454G}, TGY^{3a_E454A} and TGY^{3a_I544L}. These variants were tested on HeLa NT cells for
148 lysis. The results demonstrated that the single amino acid change at position 454 restored the
149 toxin's lytic activity (**Fig 2A**), while the amino acid change in the CRM had no effect.
150 TGY^{3a_E454G} and TGY^{3a_E454A} were further tested for lysis on HeLa hCD59 KO cells, confirming
151 their cytotoxicity to still be hCD59-dependent (**Fig 2B**).
152
153 **TGY is fully dependent on both cholesterol and hCD59**
154
155 Of the known hCD59-dependent CDCs, only ILY is completely non-functional in the absence of
156 hCD59 – it requires hCD59 to initiate binding to a host cell, though interaction with cholesterol
157 is still necessary for the subsequent steps of pore formation (34, 35). In contrast, VLY can bind
158 host cell membrane cholesterol in the absence of hCD59 (though less efficiently than binding
159 hCD59) (36), and LLY is similar (37). To assess whether TGY requires cholesterol in a manner

160 similar to ILY or VLY/LLY, HeLa cells were depleted of cholesterol using methyl-ß-cyclodextrin
161 (MßCD) and tested with TGY variants for lysis (**Fig 3A and 3B**). For comparison, similar assays
162 were conducted with ILY (fully hCD59-dependent), VLY (partially hCD59-dependent), and
163 pneumolysin (PLY; a non-specific CDC) (**Fig 3C, 3D, and 3E**).
164
165 Our results show that ILY does not lyse HeLa hCD59 KO cells but remains active on cholesterol
166 depleted HeLa cells at higher toxin concentrations. VLY, as a partially hCD59-dependent CDC,
167 lyses both HeLa hCD59 KO cells and cholesterol depleted HeLa cells at higher toxin
168 concentrations. PLY, as a non-specific CDC, lyses HeLa hCD59 KO cells at similar levels as HeLa
169 NT cells, but is inactive on cholesterol depleted HeLa cells. In contrast, TGY only lyses HeLa NT
170 cells and does not kill cells either lacking hCD59 or depleted of cholesterol. To ensure that
171 cholesterol depletion does not perturb hCD59 expression (and thereby indirectly affect lysis
172 results of hCD59-dependent toxins), hCD59 cell surface expression was analyzed using flow
173 cytometry (**Fig S1**). Results demonstrate that cholesterol depleted cells express similar levels of
174 hCD59 as HeLa NT cells. Taken together with the lysis data, our results suggest that TGY has a
175 distinct CDC lysis mechanism with an absolute requirement for both cholesterol and hCD59.
176
177 **TGY binding to host cells is affected by both cholesterol and hCD59 presence**
178
179 We set out to investigate sequential stages of CDC pore formation for TGY, starting with host
180 cell binding. HeLa cells were incubated with His-tagged TGY variants for flow cytometry analysis
181 (**Fig 4A**). The same experiment was also carried out with ILY, VLY and PLY (**Fig 4B**). The
182 percentage of PE-positive cells (indicating percentage of cells with detectable toxin bound to
183 their surface) and the mean fluorescence intensity (MFI – indicating the density of toxin bound)
184 for all conditions are listed in **Table 1**.
185
186 As expected, ILY bound well to cholesterol depleted cells, but not to hCD59 KO cells. VLY bound
187 cells in the absence of either cholesterol or hCD59, although more binding was detected on
188 cholesterol depleted cells than hCD59 KO cells. PLY bound well to hCD59 KO cells but showed

189 reduced binding to cholesterol depleted cells (**Fig 4B**). Since PLY is known to require cholesterol
190 for toxin function, the ~32% of PE-positive cholesterol depleted cells suggest that cholesterol
191 depletion is not completely effective; however, based on lysis data, the cholesterol depletion is
192 sufficient to block PLY-mediated lysis.
193
194 For the TGY variants (**Fig 4A**), the flow cytometry results suggest that TGY^{3a} is non-functional
195 due to a defect in host cell binding: only a small percentage of TGY^{3a}-exposed cells were PE-
196 positive. The results also indicate that the reduction in binding is due to the glutamic acid in L2
197 of TGY^{3a}, as there was a significant increase in PE fluorescence for TGY^{3a_E454G}-incubated cells
198 compared to TGY^{3a}-incubated cells, both in the percentage of PE-positive cells and the MFI.
199 Additionally, L2 of TGY^{3a} seems to mediate interaction with the host cell in a cholesterol-
200 dependent manner, as there is minimal binding of TGY^{3a_E454G} to cholesterol depleted cells.
201 This is consistent with previously published findings, which show that L2 inserts into host cell
202 membranes in a cholesterol-dependent manner (32, 33, 35). In hCD59 KO cells, TGY^{3a_E454G}
203 bound ~60% of the cells, although the significantly lower MFI (compared to TGY^{3a_E454G}-
204 incubated control cells) suggests fewer toxin units per cell. This finding suggests that
205 TGY^{3a_E454G} may bind to cholesterol before interacting with hCD59, but that hCD59 is still
206 required for pore formation and lysis, possibly by playing a role in oligomerization – the lower
207 MFI could indicate a lack of concentration of toxin monomers on the surface that occurs during
208 oligomerization.
209
210 Of note, TGY^{14} and TGY^{3a_E454G} have similar lysis curves but differentially bind to cholesterol
211 depleted cells: TGY^{14} binds to a significantly higher percentage of cholesterol depleted cells
212 than TGY^{3a_E454G} (**Fig 4A**). This could imply a higher affinity for hCD59 or a higher rate of
213 oligomerization. Furthermore, even though TGY^{14} can bind to a large percentage of cholesterol

214 depleted cells and both functional TGY variants are able to bind to ~50-60% of hCD59 KO cells,
215 neither of those cell lines are lysed by these toxins (**Fig 3A and 3B**). Taken together, these data
216 suggest that differences in binding ability alone do not account fully for the lysis phenotypes of
217 TGY variants and that subsequent steps of pore formation also play key roles in lysis
218 differences.
219
220 **Functional TGY requires both cholesterol and hCD59 for oligomerization**
221
222 We next investigated the oligomerization of TGY on the host cell surface. HeLa cells were
223 incubated with toxins on ice, before the cells were lysed and prepared for SDS-AGE (20).
224 Glutaraldehyde was used as a cross-linker to preserve oligomer complexes and prevent them
225 from breaking down during sample preparation. For comparison, similar analyses were also
226 carried out with ILY, VLY and PLY.
227
228 The resulting western blots demonstrate oligomer "streaks" for ILY and VLY on HeLa NT and
229 HeLa hCD59 KO cells (**Fig S3A**). PLY oligomerization was only evident in both cell lines at higher
230 toxin concentrations (**Fig S3B**), which was unsurprising as the lower PLY concentration causes
231 only ~10-15% cell death in HeLa NT cells. Oligomerization was not detectable for ILY, VLY and
232 PLY on cholesterol depleted cells (**Fig S3C**).
233
234 SDS-AGE analysis with TGY showed visible oligomers for both functional TGY variants (TGY^{14}
235 and TGY^{3a_E454G}) on control cells but a lack of visible oligomers for TGY^{3a}. Moreover, depleting
236 host cells of either cholesterol or hCD59 abrogated oligomerization for both TGY^{14} and
237 TGY^{3a_E454G} (**Fig 5**). Overall, our data indicate that TGY is dependent on both cholesterol and
238 hCD59 for binding as well as oligomerization.
239
240 **hCD59-dependent CDCs show increased lysis activity, dependent on host cell hCD59**
241 **expression levels**

242

243 We observed that the concentrations of hCD59-dependent CDCs ILY, VLY and TGY required for
244 lysis differ from those of the non-specific CDC PLY. To investigate how hCD59-dependency
245 affects the overall lytic ability of CDCs, we tested various CDCs for lysis on HeLa cells (**Fig 6A and**
246 **6B**). In the non-hCD59-dependent subset, we tested PLY and inerolysin (INY) (38). In the hCD59-
247 dependent subset, we tested ILY, VLY, TGY^{3a}, TGY^{3a_E454G} and TGY^{14}. To quantify lysis,
248 nonlinear regression analysis was performed on the data to obtain IC_{50} values for each toxin
249 (**Table 2**). All functional hCD59-dependent toxins had lower IC_{50} values than non-hCD59-
250 dependent toxins on HeLa NT control cells. VLY did not behave in a fully hCD59-dependent
251 manner, lysing cells in the absence of hCD59 expression but with lower efficiency (i.e. higher
252 IC_{50} value), as previously indicated in the literature (36). Quantitatively, VLY lyses HeLa control
253 cells at concentrations comparable to ILY (a hCD59-dependent CDC), and HeLa hCD59 KO cells
254 at concentrations similar to PLY and INY (non-hCD59-dependent CDCs) (**Table 2**). These data
255 indicate the possibility that VLY may form pores in a manner similar to either hCD59-dependent
256 CDCs or non-hCD59-dependent CDCs, depending on the characteristics of the target cell. In
257 addition, our data raise the possibility that hCD59-dependency, while restricting a CDC to a
258 single species, might increase lysis efficiency on some target cells.
259

260 To investigate if these lysis results are relevant to other human cell lines, we repeated the LDH
261 release assays with various CDCs on JEG-3 cells (**Fig 6C-6D**). Once again, hCD59-dependent
262 toxins (except for TGY variants) had lower IC_{50} values than non-hCD59-dependent toxins on
263 JEG-3 NT control cells. However, ILY consistently lysed JEG-3 NT cells at IC_{50} values ~2.5 times
264 higher than HeLa NT cells, and TGY variants lysed JEG-3 NT cells at ~14-16 times higher IC_{50}
265 values than HeLa NT cells (**Table 2**).
266

267 We hypothesized that the difference in lysis efficiency of hCD59-dependent CDCs on two
268 different human cell lines could be affected by the amount of hCD59 expressed on the surface
269 of these cells. To investigate this, we analyzed the cell surface expression of hCD59 on HeLa
270 cells and JEG-3 cells using flow cytometry (**Fig 6E**). The results show that HeLa cells express ~15

271 times more hCD59 than JEG-3 cells. These data suggest that changes in hCD59 expression levels
272 between different human cell lines can potentially affect the efficiency of hCD59-dependent
273 CDC pore formation and lysis.
274
275 **hCD59-dependency results in increased efficiency of lysis by CDCs**
276
277 Since Domain 4 is the key player that controls toxin specificity (16-18), we created hybrid CDCs
278 to isolate the role of hCD59-dependency in lysis efficiency. To do this, the Domain 4 of five
279 different CDCs was attached to Domains 1-3 of PLY, a non-hCD59 dependent CDC, resulting in
280 the following: PLY-INY, PLY-ILY, PLY-VLY, PLY-TGY^{3a}, PLY- TGY^{3a_E454G} and PLY-TGY^{14}.
281
282 Lysis caused by each of the hybrid CDCs was measured in HeLa NT and HeLa hCD59 KO cells.
283 The presence of a functional hCD59-dependent Domain 4 increased lysis efficiency of PLY-ILY
284 and PLY-VLY when compared to full-length PLY, while the presence of a non-functional Domain
285 4 (PLY-TGY^{3a}) rendered the hybrid inactive. PLY- TGY^{3a_E454G} and PLY- TGY^{14} also
286 demonstrated a decrease in IC_{50} compared to full-length PLY, albeit less than PLY-ILY and PLY-
287 VLY (**Fig 7A and Table 3**). All hybrid toxins exhibited hCD59-dependency as governed by each
288 Domain 4 (**Fig 7B**). PLY-INY (with a non-hCD59-dependent Domain 4) exhibited a slight
289 decrease in IC_{50} compared to full-length PLY, which could be expected considering full-length
290 INY has a lower IC_{50} than PLY (**Table 3**). PLY-VLY notably retained the 'intermediate' nature of its
291 Domain 4 parent: it lysed HeLa NT control cells at low concentrations, and HeLa hCD59 KO cells
292 at concentrations comparable to non-hCD59-dependent PLY, as evidenced by its IC_{50} values.
293 (**Fig 7A, 7B and Table 3**). Overall, our data suggest that in most cases, while hCD59-dependency
294 restricts CDC targets to a single species, it increases the efficiency of pore formation and lysis
295 for those toxins.
296
297

298 **DISCUSSION**

299

300 Cholesterol dependent cytolysins (CDCs) act as factors in pathogenesis for a wide range of
301 disease-causing bacteria. Understanding their mechanism of action is a key step towards
302 forming therapeutic strategies against such bacteria. Our study adds to the growing knowledge
303 regarding CDCs by characterizing a novel hCD59-dependent CDC (TGY) produced by
304 *Streptococcus oralis subsp. tigurinus*, a bacterial species implicated in various infections (25,
305 26). Our data demonstrate that of the two TGY variants, TGY^{3a} is non-functional due to a
306 defective L2, which prevents it from binding to host cells and oligomerizing. Furthermore, TGY
307 is fully hCD59-dependent and fully cholesterol dependent, setting it apart from other known
308 CDCs which are generally grouped into categories based on hCD59-dependency (37, 39) but
309 none are known to be equally dependent on both cholesterol and hCD59 for lysis. Overall, TGY
310 seems to exhibit an atypical pore forming mechanism compared to CDCs such as PLY, VLY and
311 ILY.

312

313 Our flow cytometry data investigated host cell binding for various CDCs. Binding data with PLY
314 showed that cholesterol depletion for our cells was not complete, with ~30% cells still being
315 bound by PLY (a fully cholesterol dependent CDC). However, the large shift in PE fluorescence
316 for PLY on control cells versus cholesterol depleted cells, coupled with the PLY lysis data,
317 indicated the cholesterol depletion is sufficient to abolish lysis by nonspecific CDCs. For ILY and
318 VLY, ~100% of the cholesterol depleted cells are still bound by the toxins but there is a
319 reduction in MFI. This could be due to reduced oligomerization, as fewer oligomers would mean
320 less toxin detectable on the cell surfaces.

321

322 TGY^{3a} appears to be non-functional largely due to a defect in binding to host cells. TGY^{3a_E454G}
323 did not bind well to cholesterol depleted cells but could partially bind hCD59 KO cells. This is
324 unlike ILY, which is thought to bind hCD59 before cholesterol (18, 22) and, in our experiments,
325 bound well to cholesterol depleted cells but not to hCD59 KO cells. Notably, TGY^{14} bound to

326 cholesterol depleted cells much better than TGY^{3a_E454G}, though the reason for this aberration
327 is unclear.
328
329 We conducted SDS-AGE to visualize oligomerization of CDCs on host cell surfaces. Previously,
330 hCD59 dependent CDCs have been shown to require either cholesterol or hCD59 for
331 oligomerization, but not both factors together: ILY can oligomerize on cholesterol depleted cells
332 but requires hCD59 for oligomerization (22, 34, 40), while VLY has been shown to oligomerize
333 on liposomes lacking hCD59 (36). Our oligomerization assays demonstrated no visible oligomers
334 for ILY and VLY in the absence of either hCD59 or cholesterol. The oligomerization data for ILY
335 and VLY correspond to our binding data, which suggested loss of oligomers on cholesterol
336 depleted cells as discussed above. It is relevant to note, however, that all binding and
337 oligomerization data was based on a toxin concentration of 5 μg/ml, which was sufficient for
338 lysis of relevant cell lines when cells are incubated at 37°C for 1.5 hours, but might not be
339 enough for oligomerization when cells are incubated for a shorter time period on ice (as during
340 sample preparation for flow cytometry and SDS-AGE). Therefore, despite ILY and VLY lysing
341 cholesterol depleted cells, and VLY lysing hCD59 KO cells (**Fig 3 and 4**), we observe reduced
342 binding and no oligomerization.
343
344 SDS-AGE with TGY variants showed that both hCD59 and cholesterol are important for
345 oligomerization of functional TGY. Consequently, even though TGY^{3a_E454G} bound to about half
346 of hCD59 KO cells, and TGY^{14} bound partially to both cholesterol depleted cells and hCD59 KO
347 cells, no lysis was seen on these cell lines, likely due to a lack of sufficient oligomerization.
348
349 Overall, our data demonstrate that TGY residue 454 significantly affects the host cell binding,
350 modulating toxin activity. Furthermore, both cholesterol and hCD59 are required for
351 oligomerization. Our data also imply that the pore forming mechanism of TGY and its
352 interactions with hCD59 and cholesterol potentially vary from those of other hCD59-dependent
353 CDCs. It is prudent to note that the idea of an atypical CDC pore-formation mechanism is not
354 entirely unique. ILY and VLY (both hCD59-dependent CDCs) bind hCD59 differently: VLY has a

355 lower affinity for hCD59 than ILY, and its complex with hCD59 has a different conformation (18).
356 The UDP of VLY can also adopt two different conformations upon interacting with host cell
357 membrane, whereas ILY UDP consistently adopts one orientation (18). The CDC arcanolysin
358 (ALN) displays varying specificity for different mammalian cell lines in a non-hCD59-dependent
359 manner (41). There has also been recent evidence that CDCs might interact with glycans or
360 heparan sulfates on host cell surfaces (42-44). It is therefore possible that host cell factors other
361 than hCD59 and cholesterol, as well as conformational variations in the toxin structure, could
362 play roles in the TGY pore forming mechanism.
363
364 The second part of our study aimed to understand the selective pressure behind the evolution
365 of hCD59-dependency in some CDCs. Most CDCs are nonspecific, which means they can target
366 and lyse cells from different species. Conversely, hCD59-dependency restricts CDCs to targeting
367 only human cells. Furthermore, it has been speculated that as hCD59 is present on all human
368 cells, hCD59-dependency would not lead to greater specificity for a particular cell type (45). The
369 data presented in this study demonstrate that hCD59-dependent CDCs like ILY lyse HeLa cells
370 with higher efficiency than non-hCD59-dependent CDCs like PLY and INY. We also showed that
371 CDCs such as VLY behave like intermediate CDCs, lysing cells at low concentrations comparable
372 to ILY when hCD59 is accessible and at higher concentrations comparable to PLY/INY when
373 hCD59 is not available. Additionally, our data showed a difference in hCD59-dependent toxin
374 concentrations needed for lysis of HeLa cells than those needed for JEG-3 cells. This implied
375 that host factors other than the binary presence or absence of hCD59 affected lysis efficiency of
376 these toxins. Flow cytometry data for hCD59 expression on the surface of HeLa and JEG-3 cells
377 revealed a significantly lower amount of hCD59 expressed on JEG-3 cells. The fact that higher
378 concentrations of hCD59-dependent toxins are required to lyse JEG-3 cells leads to the theory
379 that while all human cells express hCD59, differing levels of hCD59 expression could allow
380 hCD59-dependent CDCs to preferentially target some cell types over others in the human body.
381
382 Understanding CDC pore-formation is an important step towards developing strategies that can
383 help mitigate PFT-driven bacterial virulence. To this end, our study adds to the growing

384 knowledge around human-specific CDCs by investigating the function of a novel hCD59-
385 dependent CDC. Furthermore, our comparative functional analysis on a range of CDCs
386 endeavors to help us understand the development of human-specificity within this broad family
387 of pore forming toxins.
388
389 **MATERIALS AND METHODS**
390
391 *Cell Culture*
392 HeLa cells (ATCC #CCL-2) and JEG-3 cells (ATCC #HTB-36) were cultivated in EMEM medium
393 supplemented with 10% heat-inactivated fetal bovine serum (FBS) and penicillin/streptomycin.
394 For cells transduced with lentivirus to create NT control cells and hCD59 KO cells, the media
395 was further supplemented with 0.9μg/ml puromycin. Cells were grown in humidified incubators
396 at 37°C and 5% CO_2.
397
398 *Generation of Knockout Cell Lines*
399 NT control and hCD59 KO cell lines were generated as previously described (31). Briefly, single
400 guide RNAs (sgRNAs) were ligated into an empty pLentiCRISPR plasmid backbone (gifted by Dr
401 Feng Zhang; *Addgene plasmid #52961* (46)) and packaged into lentivirus using XtremeGENE 9
402 DNA Transfection Reagent. Cells were transduced with the lentivirus using spinfection. To
403 generate single cell clones from polyclonal KO cell lines, limiting dilutions were performed.
404
405 *Cell Viability Assays (LDH)*
406 LDH Cytotoxicity assay (*Sigma-Aldrich 11644793001*) to measure lysis was conducted according
407 to the manufacturer's instructions. Briefly, 2.0 x 10^4 HeLa cells were seeded per well in a 96-
408 well plate overnight. For cholesterol depletion, cells were incubated with 4 mg/ml methyl-ß-
409 cyclodextrin (MßCD) for 1 hour and washed with PBS. Cells were incubated in appropriate
410 dilutions of toxin in fresh medium for 1.5 hours. 100 μl of the supernatant was transferred to a
411 new 96-well plate and 100 μl of Reaction mixture consisting of dye solution and catalyst

412 (prepared according to the manufacturer's protocol) added. Plates were incubated in the dark
413 for 30 mins. Absorbance of samples was measured at 492nm.
414
415 *Recombinant Toxins and Hybrid Toxins*
416 Hybrid toxins PLY- TGY^{3a} and PLY- TGY^{14} were created using Gibson assembly. Primers were
417 designed to isolate PLY Domains 1-3 and the Domain 4 of TGY variants using NEB Builder tool,
418 with overhangs to ensure the alignment of each Domain 4 with PLY Domain 3. The primers
419 were used to PCR amplify the relevant fragments, which were then gel-extracted. A pET28a
420 vector was double-digested using NdeI and XhoI, and gel-extracted. Gibson assembly was
421 carried out with the digested pET28a vector, PLY Domains 1-3, and TGY Domain 4. The reaction
422 product was transformed into NEB 5-alpha cells and minipreps prepared, before being
423 sequenced using T7 primers.
424
425 Recombinant PLY, INY, ILY, VLY, PLY-ILY, PLY-VLY, and PLY-INY were prepared as described (38).
426 Full-length and hybrid toxins (TGY^{3a}, TGY^{14}, TGY^{3a_E454G}, TGY^{3a_E454A}, TGY^{3a_I544L}, PLY-
427 TGY^{3a}, PLY- TGY^{3a_E454G} and PLY- TGY^{14}) were purified as follows. Briefly, the gene encoding
428 each toxin was codon-optimized for *E. coli*, cloned into pET28a, and transformed into *E. coli*
429 T7Iq. Protein expression was induced by the addition of IPTG. Cells were lysed with a lysis
430 buffer (50 mM NaH_2PO_4, 300 mM NaCl, 10 mM imidazole). The toxin was purified from the
431 lysate using HisTrap columns with an FPLC unit into elution buffer (50mM NaH_2PO_4, 300mM
432 NaCl, 250mM imidazole), then buffer exchanged into PBS using Amicon Ultra-4 filters. The
433 concentration of each toxin was measured using a Bradford Assay.
434
435 *Site-Directed Mutagenesis*
436 For mutagenesis of TGY residue 454 and 544, the New England Biolabs Q5 Site Directed
437 Mutagenesis kit (*NEB E0552S*) was used according to the manufacturer's protocols. Briefly, the
438 NEBaseChanger tool was used to generate primers to make the relevant substitutions. These
439 primers were used to PCR amplify the mutated gene incorporated into a pET28a vector, and the

440 PCR product transformed into NEB 5-alpha cells for amplification. Minipreps were prepared and
441 sequenced to confirm the mutations, before transformation into T7Iq cells for protein
442 purification.
443
444 *Flow cytometry*
445 Flow cytometry with His-tagged toxins was carried out using direct staining. 1.0 x 10^6 cells were
446 washed and incubated with 5 μg/ml of each toxin for 10 minutes on ice. Cells were washed with
447 PBS three times and resuspended in 100 μl of ice-cold PBS + 10% FBS + 1% sodium azide.
448 Phycoerythrin (PE) anti-His tag antibody (*BioLegend 362603*) was added to the cell suspension
449 at a dilution of 1:20 and incubated for 30 minutes on ice in the dark. Cells were washed with
450 ice cold PBS, and resuspended in 300 μl of ice-cold PBS + 3% BSA + 1% sodium azide. Flow
451 cytometry to visualize hCD59 expression was carried out using indirect staining as described
452 previously (31). Stained cells were visualized on a CytoFlex Analyzer flow cytometer, and the
453 data analyzed using FlowJo software (version 10.8.1). Cells were gated as follows: live cells
454 using forward scatter area and side scatter area; single cells using forward scatter area and
455 forward scatter height; fluorescence-positive cells using PE-fluorescence intensity or AF647
456 fluorescence intensity, and forward scatter height. Samples contained at least 10,000 gated live
457 cells.
458
459 *Oligomerization western blot*
460 To visualize CDC oligomers, SDS-AGE analysis was carried out as described (20). Briefly, 1.0 x 10^6
461 cells were washed then incubated with 5 μg/ml of each toxin (or 30 μg/ml for PLY where
462 indicated) for 10 minutes on ice. Cells were washed twice with PBS and once with HEPES/NaCl
463 buffer (20 mM HEPES at pH 7.5, 150 mM NaCl), before being resuspended in 40 μl of 0.01%
464 glutaraldehyde in HEPES/NaCl as a cross-linker and incubated at 37°C for 15 minutes. 0.1M Tris
465 (pH 8.0) was added to stop the cross-linking reaction. Tris-Glycine SDS Sample buffer (*LC2676;*
466 *ThermoFisher*) was added to the cell solution at a 1:1 ratio and the mixture incubated at 95°C
467 for 20 minutes to lyse the cells.
468

469 The lysate was loaded onto a 1.5% agarose gel. Proteins from the gel were transferred to a
470 polyvinylidene difluoride (PVDF) membrane using semi-wet transfer, blocked in 5% nonfat dry
471 milk in Tris-buffered saline (TBS) plus 1% Tween-20, and incubated with 6x His-tag monoclonal
472 primary antibody (*MA1-135; ThermoFisher*) overnight at a dilution of 1:750. The membrane was
473 washed with TBS plus 1% Tween-20, and incubated with goat anti-mouse IgG secondary
474 antibody (*31430; ThermoFisher*) for 1 hour at a 1:10,000 dilution. The membrane was then
475 washed with several changes of TBS plus 1% Tween-20 for 3 hours before being imaged on
476 iBright CL1000 using Pierce ECL Western Blotting Substrate.
477

478 **ACKNOWLEDGEMENTS**
479 This work was supported by grant R01 AI155476 to AJR.

A)

```
TGY AZ_3a   TETTVSSSNLKTDAENTEKETVPSSATNNNSVDVMDSLMKATNQEGKDLNKYLFGLTYNKI   105
TGY AZ_14   TETTVSSSNLKTDAENTEKETVPSSATNNNSVDVMDSLMKATNQEDKDLNKYLFGLTYNKI

TGY AZ_3a   DILTRKGETIENYSNTSAKQQGNEFIVVEKVKKSLSNKSEDVSINGNSDIFLGALFKANQD   166
TGY AZ_14   DILTRKGETIENYSNTSAKQKGNEFIVVEKVKKSLSNKSEDVSINGNSDIFLGALFKANQD

TGY AZ_3a   LLENKPQLVSISRKPGRISVDLPGMAGADSHTDAEPTVSGMQEGINTLVNRWNEKYAANNP   227
TGY AZ_14   LLENKPQLVSISRKPGRISVDLPGMAGADSHTDAEPTVSGMQEGINTLVNRWNEKYAANNP

TGY AZ_3a   APARMHYESTSAYSMNQLKAKFGSDFEKVGANLKIDFEAAQKGEKQIEVVDFKQVYYTANF   288
TGY AZ_14   APARMQYESTSAYSMNQLKAKFGSDFEKVGANLKIDFEAAQKGEKQIEVVDFKQVYYTANF

TGY AZ_3a   DAPKNPSDVFGDDVTVKDLQDRGLDNQTPPVYVSSVSYGRQMYVKFETTSTSTELKAAINA   349
TGY AZ_14   DAPKNPSDVFGDDVTVKDLQDRGLDNQTPPVYVSSVSYGRQMYVKFETTSTSTELKAAINA

TGY AZ_3a   VIKGVPINPESEWARVLKNTSVTAAIVGGNADGAARVVTGTAEDLKKLIQEGANFSTQNPA   410
TGY AZ_14   VIKGVPINPESEWARVLKNTSVTAAIVGGNADGAARVVTGTAEDLKKLIQEGANFSTQNPA

TGY AZ_3a   VPVSYKTAFLRDNQVATIQSSTDYIETKVTSYKNGYLNLHHKGEYVARYYIYWDEVTYDED   471
TGY AZ_14   VPVSYKTAFLRDNQVATIQSSTDYIETKVTSYKNGYLNLHHKGGYVARYYIYWDEVTYDED

TGY AZ_3a   GIESIRSREWEDNGKNRTSGFQTELQFRGNVRNIRVKIQEKTGLAWEPWRTVYYRTELPLV   532
TGY AZ_14   GIESIRSREWEDNGKNRTSGFQTELQFRGNVRNLRVKIQEKTGLAWEPWRTVYYRTELPLV

TGY AZ_3a   QKRTITNYGTTIRPKYTEEIENN   555
TGY AZ_14   QKRTITNYGTTIRPKYTEEIENN
```

B)

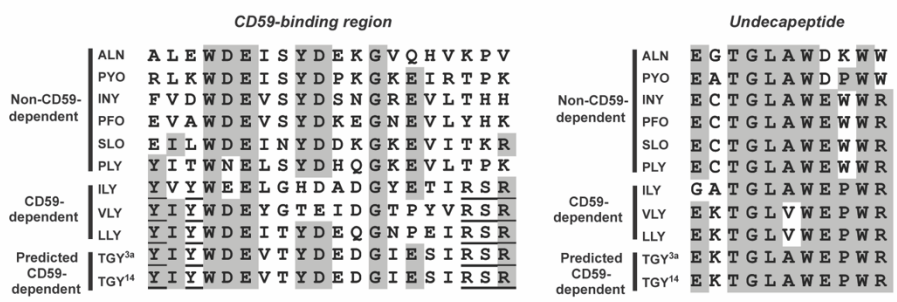

C)

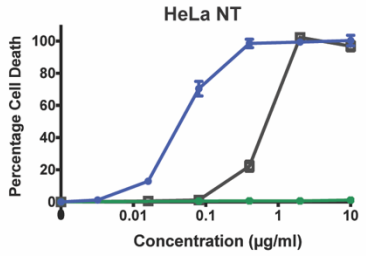

D)

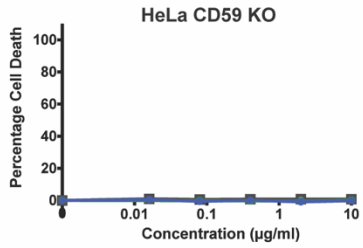

TGY3a TGY14 ILY

E)

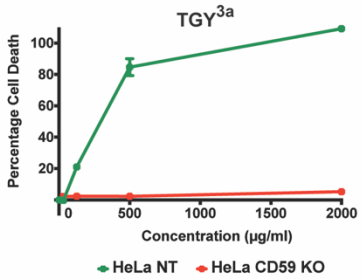

481 **Figure 1: Two variants of novel CDC tigurilysin (TGY) exist, with differing lysis activity**
482 (**A**) The predicted amino acid sequences of the two mature TGY variants. The signal sequence
483 comprising the first 44 amino acids, as predicted by SignalP 5.0 (SignalP 5.0 - DTU Health Tech -
484 Bioinformatic Services), was eliminated from the sequences shown here. There are 5 single
485 amino acid differences (shaded) between TGY^{3a} and TGY^{14}. The last two (amino acid 454 and
486 amino acid 544) are found in domain 4.
487 (**B**) Left panel: the conserved hCD59-binding sequence (Y-X-Y-X14-R-S-R; underlined) in Domain
488 4 of various hCD59-dependent CDCs, as compared to the same region of non-hCD59-dependent
489 CDCs. Right panel: The conserved 11-amino acid sequence (undecapeptide), necessary for CDC
490 interaction with cholesterol and subsequent pore formation, as found in various CDCs. The
491 proline at the 9th position is conserved among hCD59-dependent CDCs. The shaded regions in
492 both panels show the consensus sequence as determined by MacVector.
493 (**C-D**) Percentage cell death in HeLa NT control cells and HeLa hCD59 KO cells when exposed to
494 increasing concentrations of TGY^{3a} and TGY^{14}, with ILY for comparison as a known hCD59-
495 dependent CDC. Cells were incubated with toxins for 1.5 hours and cell death measured by an
496 LDH-release cytotoxicity assay. Each point is the mean of 3 replicates, and error bars represent
497 ±SD.
498 (**E**) Percentage cell death in HeLa NT control cells and HeLa hCD59 KO cells when exposed to
499 supraphysical concentrations of TGY^{3a}. Cells were incubated with toxin for 1.5 hours and cell
500 death measured by an LDH-release cytotoxicity assay. Each point is the mean of 3 replicates,
501 and error bars represent ±SD.
502
503
504

505

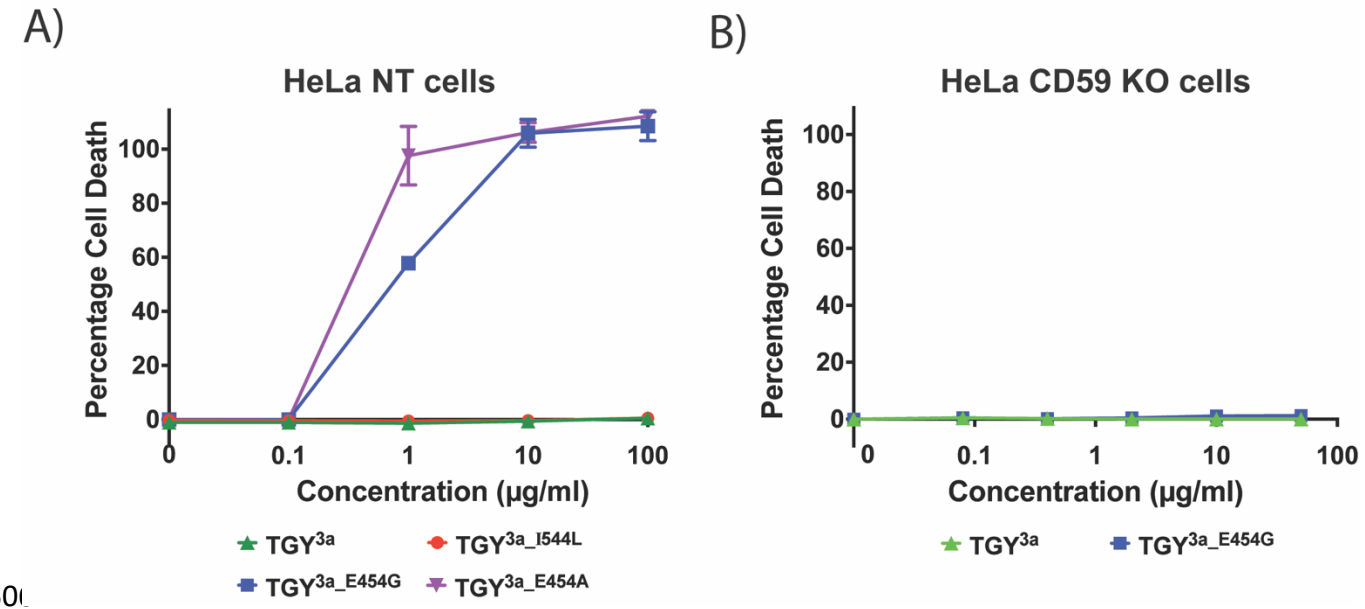

506
507
508 **Figure 2: A glutamic acid-to-glycine change at position 454 affects TGY activity**
509 (**A**) Percentage cell death in HeLa NT control cells when exposed to increasing concentrations of
510 TGY^{3a} and its mutagenized counterparts. Only the amino acid change at position 454 (glutamic
511 acid to glycine or alanine) restored toxin functionality. Cells were incubated with toxins for 1.5
512 hours and cell death measured by an LDH-release cytotoxicity assay. Each point is the mean of 3
513 replicates, and error bars represent ±SD.
514 (**B**) Percentage cell death in HeLa hCD59 KO cells when exposed to increasing concentrations of
515 TGY^{3a} and TGY^{3a_E454G}, to determine if the toxins are hCD59-dependent. Cells were incubated
516 with the toxins for 1.5 hours and cell death measured by an LDH-release cytotoxicity assay.
517 Each point is the mean of 3 replicates, and error bars represent ±SD.
518
519

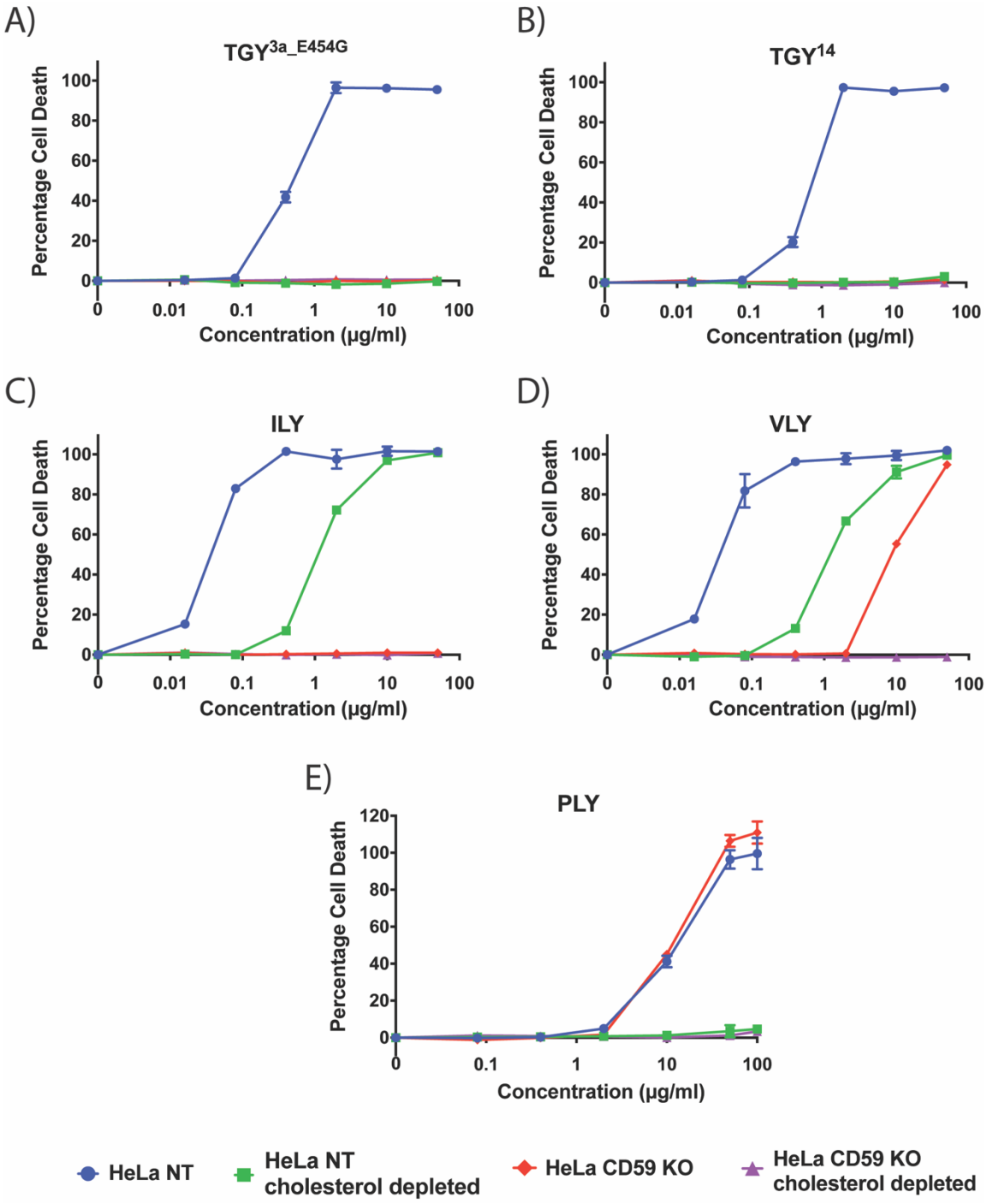

Figure 3: Functional TGY is fully cholesterol dependent.

(**A-E**) Percentage cell death in HeLa NT control cells, HeLa hCD59 KO cells, HeLa cholesterol depleted cells, and HeLa hCD59 KO + cholesterol depleted cells. Cells were exposed to a range of concentrations of each toxin for 1.5 hours, and cell death measured by an LDH-release cytotoxicity assay. Each point is the mean of 3 replicates, and error bars represent ±SD.

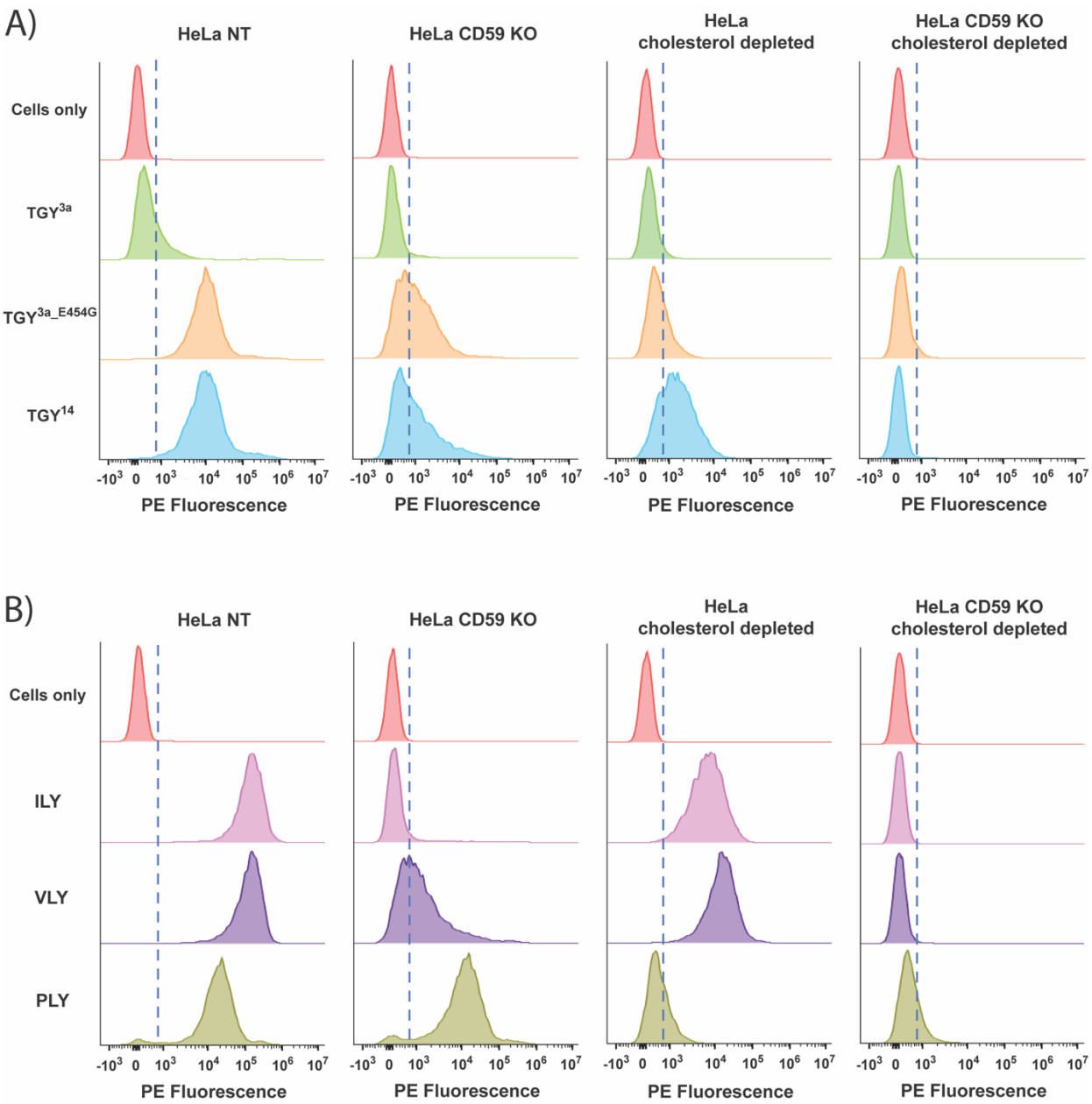

<u>Figure 4: TGY3a is defective in host cell binding, while functional TGY is dependent on both cholesterol and hCD59 for host cell binding.</u>

(**A-B**) Flow cytometry analysis of His-tag expression on the cell surface after HeLa cells (NT control, hCD59 KO, cholesterol depleted, and hCD59 KO + cholesterol depleted) were incubated with His-tagged toxins, before addition of a PE anti-His-tag antibody. Histogram x-axis shows fluorescence intensity of the PE-conjugated antibody for each cell population. Histogram y-axis shows cell count normalized to mode. The dotted line demarcates the PE-negative cells and the PE-positive cells, based on the fluorescence intensity of control cells not incubated with any toxin.

542

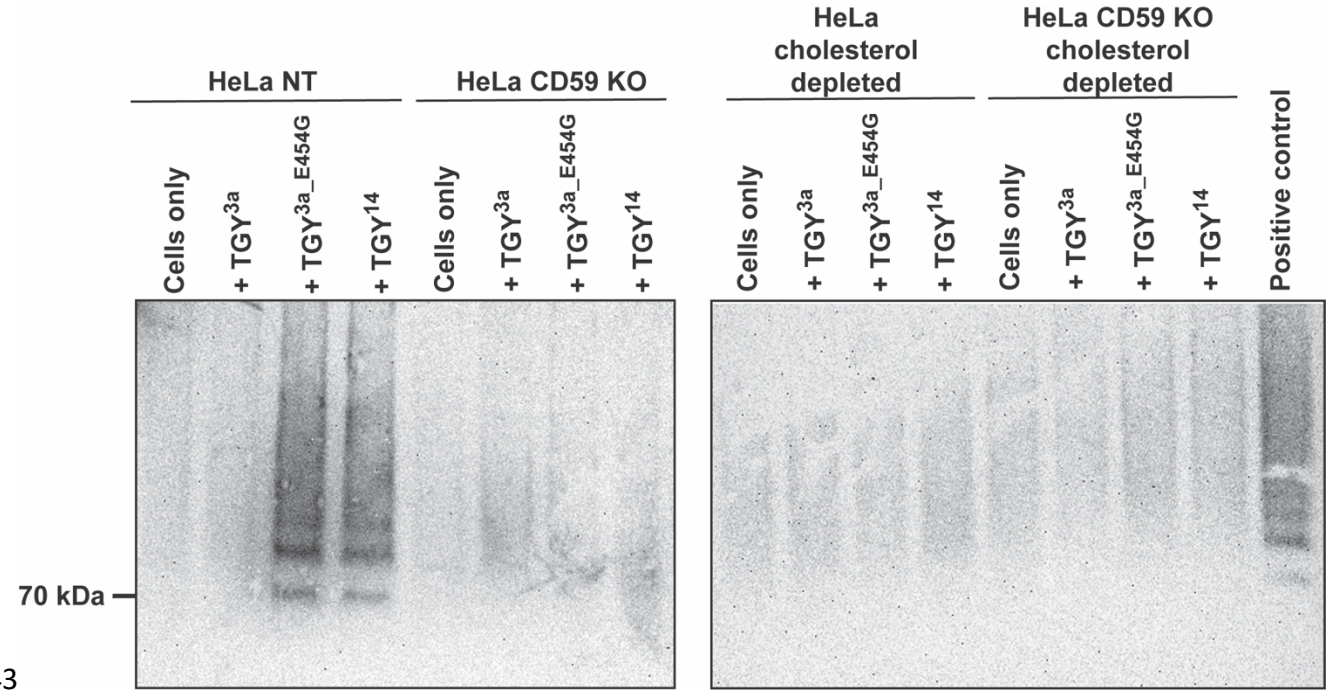

543
544
545
546 **Figure 5: Functional TGY is dependent on both cholesterol and hCD59 for oligomerization on**
547 **host cell surface.**
548 Oligomerization of TGY variants as assessed by SDS-AGE analysis. Cells were incubated with the
549 indicated toxins on ice before being prepared for western blotting. 0.01% glutaraldehyde was
550 used as a cross-linker to preserve oligomers during sample preparation. Western blot
551 membrane was probed with an anti-His-tag HRP-conjugated antibody.
552

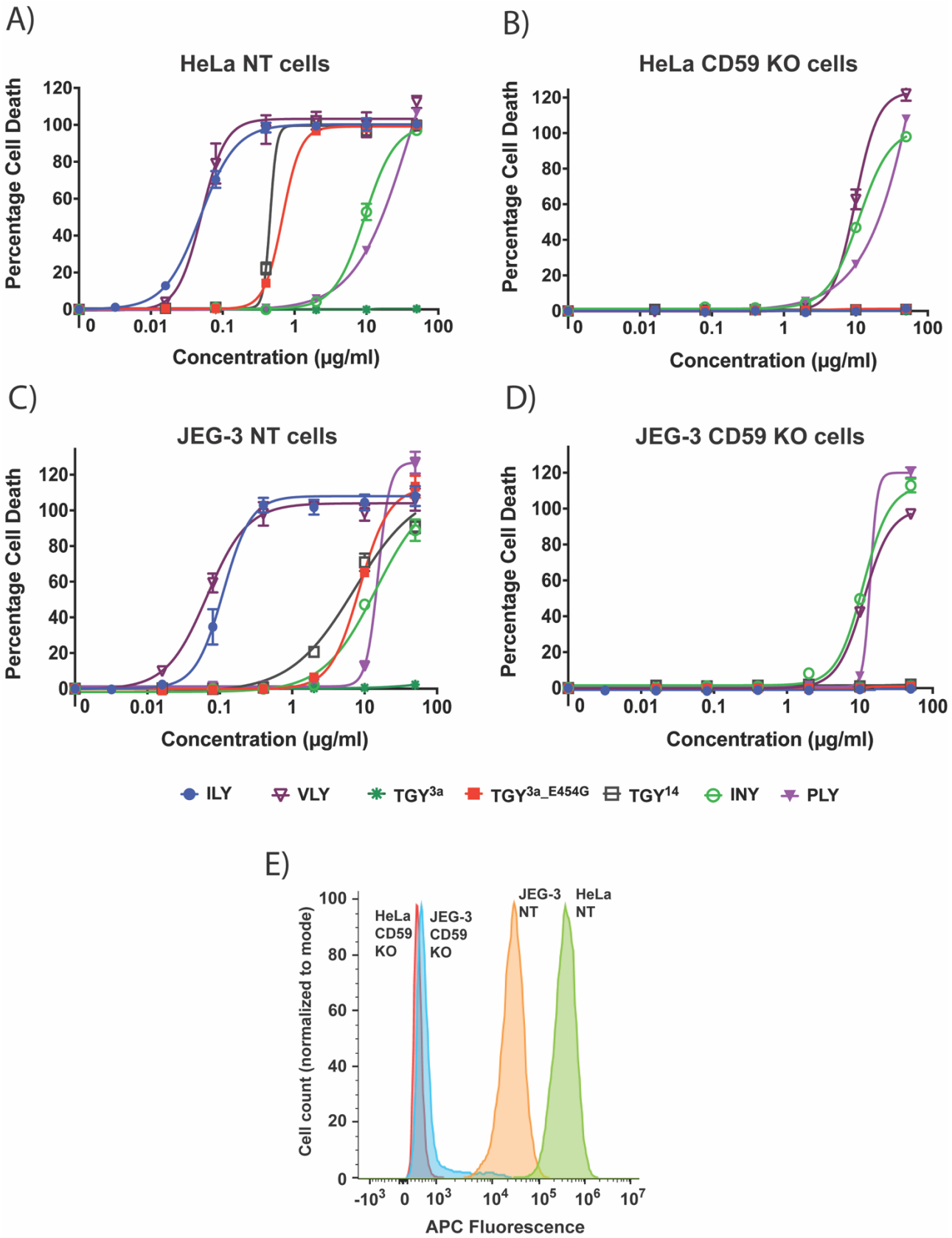
A)
HeLa NT cells
Percentage Cell Death
Concentration (µg/ml)
B)
HeLa CD59 KO cells
Percentage Cell Death
Concentration (µg/ml)
C)
JEG-3 NT cells
Percentage Cell Death
Concentration (µg/ml)
D)
JEG-3 CD59 KO cells
Percentage Cell Death
Concentration (µg/ml)
ILY
VLY
TGY3a
TGY3a_E454G
TGY14
INY
PLY
E)
HeLa CD59 KO
JEG-3 CD59 KO
JEG-3 NT
HeLa NT
Cell count (normalized to mode)
APC Fluorescence

553
554

Figure 6: hCD59-dependency coupled with high hCD59 expression increases CDC ability to lyse cells at lower concentrations

(**A-B**) Percentage cell death in HeLa NT control cells and HeLa hCD59 KO cells when exposed to various full-length CDCs, both hCD59-dependent and non-hCD59-dependent. Cells were incubated with toxins for 1.5 hours and cell death measured by an LDH-release cytotoxicity assay. Each point is the mean of 3 replicates, and error bars represent ±SD.

(**C-D**) Percentage cell death in JEG-3 NT control cells and JEG-3 hCD59 KO cells when exposed to various full-length CDCs, both hCD59-dependent and non-hCD59-dependent. Cells were incubated with toxins for 1.5 hours and cell death measured by an LDH-release cytotoxicity assay. Each point is the mean of 3 replicates, and error bars represent ±SD.

(**E**) Flow cytometry analysis of hCD59 expression on the cell surface for HeLa cells and JEG-3 cells. Cells were incubated with a primary anti-hCD59 mouse IgG2a antibody and a secondary anti-mouse IgG2a AF647 antibody. Histogram x-axis shows fluorescence intensity of the APC-conjugated secondary antibody for each cell population. Histogram y-axis shows cell count normalized to mode.

Abbreviations: ILY, intermedilysin; VLY, vaginolysin; TGY, tigurilysin; INY, inerolysin; PLY, pneumolysin.

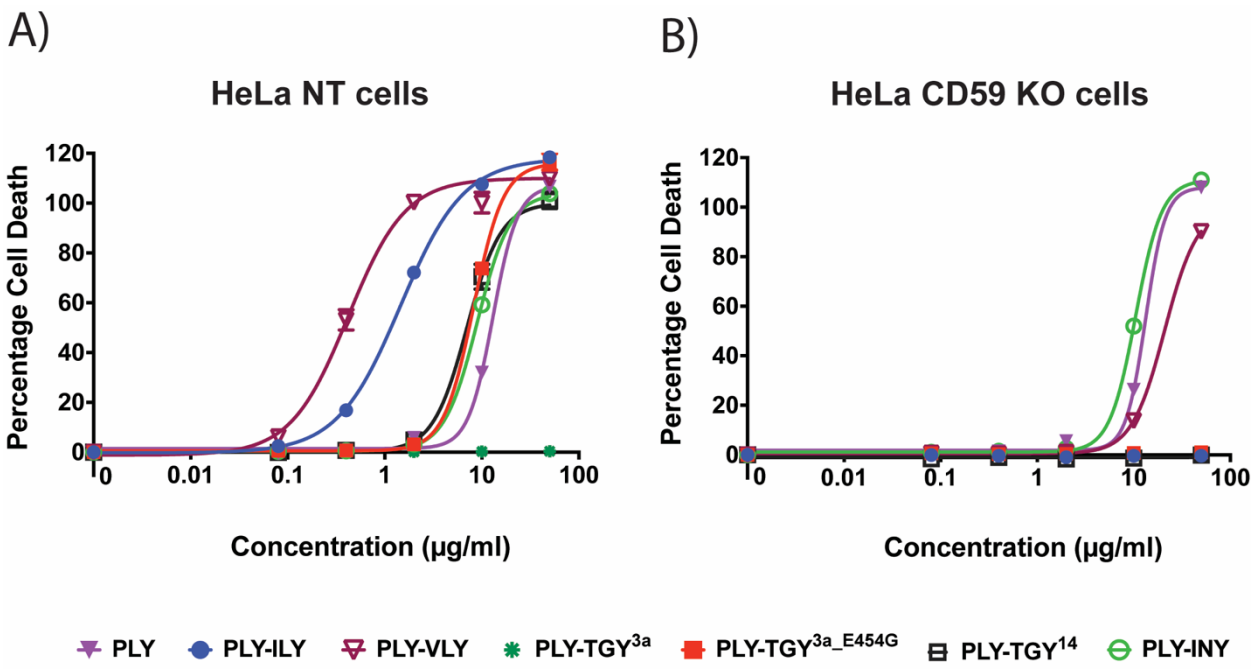

574
575
576
577 **Figure 7: Incorporating a hCD59-dependent Domain 4 increases CDC ability to lyse cells at**
578 **lower concentrations**
579 (**A-B**) Percentage cell death in HeLa NT control cells and HeLa hCD59 KO cells when exposed to
580 various PLY-hybrid CDCs, with both hCD59-dependent and non-hCD59-dependent D4s. Cells
581 were incubated with toxins for 1.5 hours and cell death measured by an LDH-release
582 cytotoxicity assay. Each point is the mean of 3 replicates, and error bars represent ±SD.
583

	% PE-positive cells	MFI values
HeLa NT cells only	1	112
HeLa hCD59 KO cells only	1	578
HeLa NT cholesterol depleted cells only	0	136
HeLa hCD59 KO cholesterol depleted cells only	1	138
HeLa NT + ILY	100	170246
HeLa hCD59 KO + ILY	11	6767
HeLa NT cholesterol depleted + ILY	99	9910
HeLa hCD59 KO cholesterol depleted + ILY	1	151
HeLa NT + VLY	100	150828
HeLa hCD59 KO + VLY	65	8167
HeLa NT cholesterol depleted + VLY	100	21252
HeLa hCD59 KO cholesterol depleted + VLY	2	181
HeLa NT + PLY	96	30816
HeLa hCD59 KO + PLY	95	23677
HeLa NT cholesterol depleted + PLY	32	697
HeLa hCD59 KO cholesterol depleted + PLY	24	625
HeLa NT + TGY^{3a}	28	9735
HeLa hCD59 KO + TGY^{3a}	6	335
HeLa NT cholesterol depleted + TGY^{3a}	7	4261
HeLa hCD59 KO cholesterol depleted + TGY^{3a}	1	598
HeLa NT + TGY^{3a_E454G}	99	28460
HeLa hCD59 KO + TGY^{3a_E454G}	60	3813
HeLa NT cholesterol depleted + TGY^{3a_E454G}	34	3847
HeLa hCD59 KO cholesterol depleted + TGY^{3a_E454G}	8	281
HeLa NT + TGY^{14}	99	31109
HeLa hCD59 KO + TGY^{14}	54	4126

HeLa NT cholesterol depleted + TGY[14]	79	2380
HeLa hCD59 KO cholesterol depleted + TGY[14]	2	232

584
585
586 **Table 1: Quantification of Flow Cytometry Data of CDC Binding on HeLa cells**
587 The percentage of PE-positive live cells were calculated by FlowJo based on gating of PE-
588 negative cells as determined by cells-only controls. The MFI for each sample was calculated by
589 FlowJo for cells gated as live cells → single cells.
590
591
592
593
594
595
596
597
598
599
600
601
602
603
604
605
606
607
608
609
610
611
612
613
614
615
616
617
618
619
620
621

	IC_{50} on HeLa NT control cells (µg/ml)	IC_{50} on HeLa hCD59 KO cells (µg/ml)	IC_{50} ratio HeLa hCD59 KO : HeLa NT	IC_{50} on JEG-3 NT control cells (µg/ml)	IC_{50} on JEG-3 hCD59 KO cells (µg/ml)	IC_{50} ratio JEG-3 hCD59 KO : JEG-3 NT
ILY	0.03 ± 0.01	*ND*	*NA*	0.08 ± 0.01	*ND*	*NA*
VLY	0.04 ± 0.01	8.92 ± 1.61	223.0	0.05 ± 0.03	10.73 ± 0.65	214.6
TGY^{3a}	*ND*	*ND*	*NA*	*ND*	*ND*	*NA*
TGY^{3a_E454G}	0.50 ± 0.18	*ND*	*NA*	7.04 ± 1.14	*ND*	*NA*
TGY^{14}	0.46 ± 0.04	*ND*	*NA*	7.56 ± 4.41	*ND*	*NA*
INY	8.12 ± 3.74	8.26 ± 3.52	1.0	12.98 ± 1.95	9.99 ± 0.13	0.7
PLY	15.46 ± 4.41	17.26 ± 5.34	1.1	10.89 ± 0.95	10.48 ± 2.77	1.0

622
623
624 **Table 2: IC_{50} values of CDCs tested for lysis on HeLa and JEG-3 cells.**
625 Full-length CDCs were tested for lysis on the indicated cell lines at a range of 0.08 µg/ml to 50
626 µg/ml, and IC_{50} values indicate the concentrations required for 50% lysis on each cell line. Each
627 IC_{50} value average with standard deviation is calculated from 3 experimental repeats. "ND"
628 indicates where the CDC did not cause any cell lysis; "NA" indicates where the IC_{50} ratio could
629 not be calculated.
630

	IC_{50} on HeLa NT control cells (µg/ml)	**IC_{50} on HeLa hCD59 KO cells (µg/ml)**	**IC_{50} ratio HeLa hCD59 KO : HeLa NT**
PLY	15.46 ± 4.41	17.26 ± 5.34	1.1
PLY-ILY	1.82 ± 0.69	*ND*	*NA*
PLY-VLY	0.67 ± 0.26	37.60 ± 16.80	56.1
PLY-TGY^{3a}	*ND*	*ND*	*NA*
PLY-TGY^{3a_E454G}	9.48 ± 0.79	*ND*	*NA*
PLY-TGY^{14}	11.26 ± 3.73	*ND*	*NA*
PLY-INY	8.66 ± 0.53	9.69 ± 0.44	1.2

631

632 **Table 3: IC_{50} values of hybrid CDCs tested for lysis on HeLa cells.**

633 Hybrid CDCs with PLY D1-3 were tested for lysis on the indicated cell lines at a range of 0.08
634 µg/ml to 50 µg/ml, and IC_{50} values indicate the concentrations required for 50% lysis on each
635 cell line. Full-length PLY IC_{50} values are included for comparison. Each IC_{50} value average with
636 standard deviation is calculated from 3 experimental repeats. "ND" indicates where the CDC did
637 not cause any cell lysis; "NA" indicates where the IC_{50} ratio could not be calculated.

638

639 **REFERENCES**

640

641 1. Gonzalez MR, Bischofberger M, Pernot L, van der Goot FG, Freche B. 2008. Bacterial
642 pore-forming toxins: the (w)hole story? Cell Mol Life Sci 65:493-507.
643 2. Stanley SA, Raghavan S, Hwang WW, Cox JS. 2003. Acute infection and macrophage
644 subversion by Mycobacterium tuberculosis require a specialized secretion system. Proc
645 Natl Acad Sci U S A 100:13001-6.
646 3. Hensler ME, Liu GY, Sobczak S, Benirschke K, Nizet V, Heldt GP. 2005. Virulence role of
647 group B Streptococcus beta-hemolysin/cytolysin in a neonatal rabbit model of early-
648 onset pulmonary infection. J Infect Dis 191:1287-91.
649 4. Orihuela CJ, Gao G, Francis KP, Yu J, Tuomanen EI. 2004. Tissue-specific contributions of
650 pneumococcal virulence factors to pathogenesis. J Infect Dis 190:1661-9.
651 5. Geny B, Popoff MR. 2006. Bacterial protein toxins and lipids: pore formation or toxin
652 entry into cells. Biol Cell 98:667-78.
653 6. Lim JH, Stirling B, Derry J, Koga T, Jono H, Woo CH, Xu H, Bourne P, Ha UH, Ishinaga H,
654 Xu H, Andalibi A, Feng XH, Zhu H, Huang Y, Zhang W, Weng X, Yan C, Yin Z, Briles DE,
655 Davis RJ, Flavell RA, Li JD. 2007. Tumor suppressor CYLD regulates acute lung injury in
656 lethal Streptococcus pneumoniae infections. Immunity 27:349-60.
657 7. Inoshima I, Inoshima N, Wilke GA, Powers ME, Frank KM, Wang Y, Bubeck Wardenburg
658 J. 2011. A Staphylococcus aureus pore-forming toxin subverts the activity of ADAM10 to
659 cause lethal infection in mice. Nat Med 17:1310-4.
660 8. Ratner AJ, Aguilar JL, Shchepetov M, Lysenko ES, Weiser JN. 2007. Nod1 mediates
661 cytoplasmic sensing of combinations of extracellular bacteria. Cell Microbiol 9:1343-51.
662 9. Collier RJ. 2009. Membrane translocation by anthrax toxin. Mol Aspects Med 30:413-22.
663 10. Los FC, Randis TM, Aroian RV, Ratner AJ. 2013. Role of pore-forming toxins in bacterial
664 infectious diseases. Microbiol Mol Biol Rev 77:173-207.
665 11. Tweten RK. 2005. Cholesterol-dependent cytolysins, a family of versatile pore-forming
666 toxins. Infect Immun 73:6199-209.
667 12. Hotze EM, Le HM, Sieber JR, Bruxvoort C, McInerney MJ, Tweten RK. 2013. Identification
668 and characterization of the first cholesterol-dependent cytolysins from Gram-negative
669 bacteria. Infect Immun 81:216-25.
670 13. Olofsson A, Hebert H, Thelestam M. 1993. The projection structure of perfringolysin O
671 (Clostridium perfringens theta-toxin). FEBS Lett 319:125-7.
672 14. Bhakdi S, Tranum-Jensen J, Sziegoleit A. 1985. Mechanism of membrane damage by
673 streptolysin-O. Infect Immun 47:52-60.
674 15. Rossjohn J, Feil SC, McKinstry WJ, Tweten RK, Parker MW. 1997. Structure of a
675 cholesterol-binding, thiol-activated cytolysin and a model of its membrane form. Cell
676 89:685-92.
677 16. Polekhina G, Giddings KS, Tweten RK, Parker MW. 2005. Insights into the action of the
678 superfamily of cholesterol-dependent cytolysins from studies of intermedilysin. Proc
679 Natl Acad Sci U S A 102:600-5.
680 17. Wickham SE, Hotze EM, Farrand AJ, Polekhina G, Nero TL, Tomlinson S, Parker MW,
681 Tweten RK. 2011. Mapping the intermedilysin-human CD59 receptor interface reveals a

682 deep correspondence with the binding site on CD59 for complement binding proteins
683 C8alpha and C9. J Biol Chem 286:20952-62.
684 18. Lawrence SL, Gorman MA, Feil SC, Mulhern TD, Kuiper MJ, Ratner AJ, Tweten RK,
685 Morton CJ, Parker MW. 2016. Structural Basis for Receptor Recognition by the Human
686 CD59-Responsive Cholesterol-Dependent Cytolysins. Structure 24:1488-98.
687 19. Shatursky O, Heuck AP, Shepard LA, Rossjohn J, Parker MW, Johnson AE, Tweten RK.
688 1999. The mechanism of membrane insertion for a cholesterol-dependent cytolysin: a
689 novel paradigm for pore-forming toxins. Cell 99:293-9.
690 20. Shepard LA, Shatursky O, Johnson AE, Tweten RK. 2000. The mechanism of pore
691 assembly for a cholesterol-dependent cytolysin: formation of a large prepore complex
692 precedes the insertion of the transmembrane beta-hairpins. Biochemistry 39:10284-93.
693 21. Czajkowsky DM, Hotze EM, Shao Z, Tweten RK. 2004. Vertical collapse of a cytolysin
694 prepore moves its transmembrane beta-hairpins to the membrane. EMBO J 23:3206-15.
695 22. Giddings KS, Zhao J, Sims PJ, Tweten RK. 2004. Human CD59 is a receptor for the
696 cholesterol-dependent cytolysin intermedilysin. Nat Struct Mol Biol 11:1173-8.
697 23. Gelber SE, Aguilar JL, Lewis KL, Ratner AJ. 2008. Functional and phylogenetic
698 characterization of Vaginolysin, the human-specific cytolysin from Gardnerella vaginalis.
699 J Bacteriol 190:3896-903.
700 24. Tabata A, Matsumoto A, Fujimoto A, Ohkura K, Ikeda T, Oda H, Yokohata S, Kobayashi
701 M, Tomoyasu T, Takao A, Ohkuni H, Nagamune H. 2022. Dual functions of
702 discoidinolysin, a cholesterol-dependent cytolysin with N-terminal discoidin domain
703 produced from Streptococcus mitis strain Nm-76. J Oral Microbiol 14:2105013.
704 25. Zbinden A, Mueller NJ, Tarr PE, Eich G, Schulthess B, Bahlmann AS, Keller PM,
705 Bloemberg GV. 2012. Streptococcus tigurinus, a novel member of the Streptococcus
706 mitis group, causes invasive infections. J Clin Microbiol 50:2969-73.
707 26. Zbinden A, Mueller NJ, Tarr PE, Sproer C, Keller PM, Bloemberg GV. 2012. Streptococcus
708 tigurinus sp. nov., isolated from blood of patients with endocarditis, meningitis and
709 spondylodiscitis. Int J Syst Evol Microbiol 62:2941-2945.
710 27. Bourassa L, Clarridge JE, 3rd. 2015. Clinical Significance and Characterization of
711 Streptococcus tigurinus Isolates in an Adult Population. J Clin Microbiol 53:3574-9.
712 28. Kanamori H, Kakuta R, Yano H, Suzuki T, Gu Y, Oe C, Inomata S, Aoyagi T, Hatta M, Endo
713 S, Tokuda K, Weber DJ, Nakamura Y, Saiki Y, Kaku M. 2015. A case of culture-negative
714 endocarditis due to Streptococcus tigurinus. J Infect Chemother 21:138-40.
715 29. Diene SM, Francois P, Zbinden A, Entenza JM, Resch G. 2016. Comparative Genomics
716 Analysis of Streptococcus tigurinus Strains Identifies Genetic Elements Specifically and
717 Uniquely Present in Highly Virulent Strains. PLoS One 11:e0160554.
718 30. Johnson S, Brooks NJ, Smith RA, Lea SM, Bubeck D. 2013. Structural basis for recognition
719 of the pore-forming toxin intermedilysin by human complement receptor CD59. Cell Rep
720 3:1369-77.
721 31. Shahi I, Llaneras CN, Perelman SS, Torres VJ, Ratner AJ. 2022. Genome-Wide CRISPR-
722 Cas9 Screen Does Not Identify Host Factors Modulating Streptococcus agalactiae beta-
723 Hemolysin/Cytolysin-Induced Cell Death. Microbiol Spectr 10:e0218621.

724 32. Ramachandran R, Heuck AP, Tweten RK, Johnson AE. 2002. Structural insights into the
725 membrane-anchoring mechanism of a cholesterol-dependent cytolysin. Nat Struct Biol
726 9:823-7.
727 33. Soltani CE, Hotze EM, Johnson AE, Tweten RK. 2007. Structural elements of the
728 cholesterol-dependent cytolysins that are responsible for their cholesterol-sensitive
729 membrane interactions. Proc Natl Acad Sci U S A 104:20226-31.
730 34. Giddings KS, Johnson AE, Tweten RK. 2003. Redefining cholesterol's role in the
731 mechanism of the cholesterol-dependent cytolysins. Proc Natl Acad Sci U S A
732 100:11315-20.
733 35. Soltani CE, Hotze EM, Johnson AE, Tweten RK. 2007. Specific protein-membrane
734 contacts are required for prepore and pore assembly by a cholesterol-dependent
735 cytolysin. J Biol Chem 282:15709-16.
736 36. Zilnyte M, Venclovas C, Zvirbliene A, Pleckaityte M. 2015. The cytolytic activity of
737 vaginolysin strictly depends on cholesterol and is potentiated by human CD59. Toxins
738 (Basel) 7:110-28.
739 37. Tabata A, Ohkura K, Ohkubo Y, Tomoyasu T, Ohkuni H, Whiley RA, Nagamune H. 2014.
740 The diversity of receptor recognition in cholesterol-dependent cytolysins. Microbiol
741 Immunol 58:155-71.
742 38. Rampersaud R, Planet PJ, Randis TM, Kulkarni R, Aguilar JL, Lehrer RI, Ratner AJ. 2011.
743 Inerolysin, a cholesterol-dependent cytolysin produced by Lactobacillus iners. J Bacteriol
744 193:1034-41.
745 39. Tomoyasu T, Matsumoto A, Takao A, Tabata A, Nagamune H. 2023. A simple method to
746 differentiate three classes of cholesterol-dependent cytolysins. J Microbiol Methods
747 207:106696.
748 40. Boyd CM, Parsons ES, Smith RA, Seddon JM, Ces O, Bubeck D. 2016. Disentangling the
749 roles of cholesterol and CD59 in intermedilysin pore formation. Sci Rep 6:38446.
750 41. Jost BH, Lucas EA, Billington SJ, Ratner AJ, McGee DJ. 2011. Arcanolysin is a cholesterol-
751 dependent cytolysin of the human pathogen Arcanobacterium haemolyticum. BMC
752 Microbiol 11:239.
753 42. Shewell LK, Day CJ, Jen FE, Haselhorst T, Atack JM, Reijneveld JF, Everest-Dass A, James
754 DBA, Boguslawski KM, Brouwer S, Gillen CM, Luo Z, Kobe B, Nizet V, von Itzstein M,
755 Walker MJ, Paton AW, Paton JC, Torres VJ, Jennings MP. 2020. All major cholesterol-
756 dependent cytolysins use glycans as cellular receptors. Sci Adv 6:eaaz4926.
757 43. Shewell LK, Harvey RM, Higgins MA, Day CJ, Hartley-Tassell LE, Chen AY, Gillen CM,
758 James DB, Alonzo F, 3rd, Torres VJ, Walker MJ, Paton AW, Paton JC, Jennings MP. 2014.
759 The cholesterol-dependent cytolysins pneumolysin and streptolysin O require binding to
760 red blood cell glycans for hemolytic activity. Proc Natl Acad Sci U S A 111:E5312-20.
761 44. Drabavicius G, Daelemans D. 2021. Intermedilysin cytolytic activity depends on heparan
762 sulfates and membrane composition. PLoS Genet 17:e1009387.
763 45. Johnstone BA, Joseph R, Christie MP, Morton CJ, McGuiness C, Walsh JC, Bocking T,
764 Tweten RK, Parker MW. 2022. Cholesterol-dependent cytolysins: The outstanding
765 questions. IUBMB Life 74:1169-1179.
766 46. Sanjana NE, Shalem O, Zhang F. 2014. Improved vectors and genome-wide libraries for
767 CRISPR screening. Nat Methods 11:783-784.

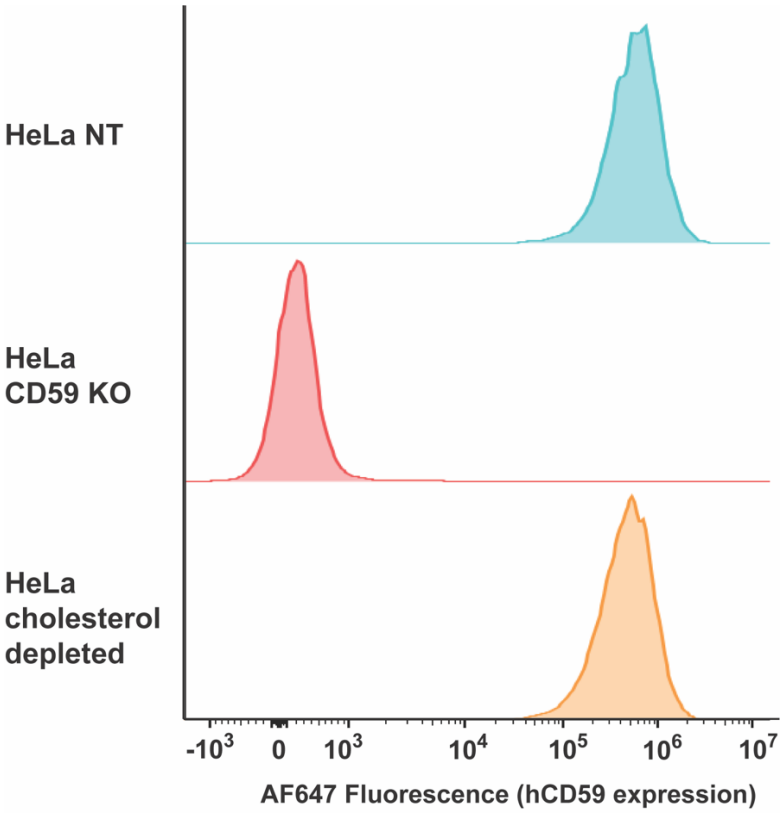

768
769
770
771 **Figure S1: Cholesterol depletion does not affect hCD59 expression on HeLa cell surface**
772 Flow cytometry analysis of hCD59 expression on the cell surfaces of HeLa cells (NT control,
773 hCD59 KO, and cholesterol depleted) using an anti-hCD59 primary antibody and an Alexa-Fluor
774 647 (AF647) secondary antibody. Histogram x-axis shows APC fluorescence intensity of the
775 secondary antibody for each cell population. Histogram y-axis shows cell count normalized to
776 mode.
777

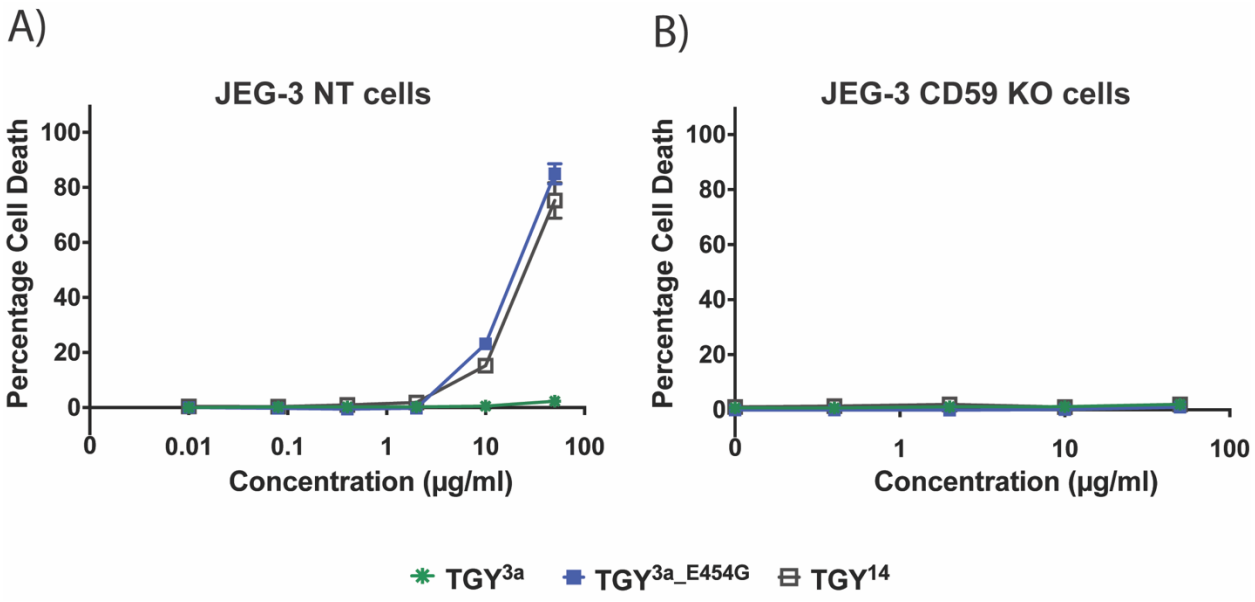

Figure S2: Functional TGY variants lyse JEG-3 cells in a hCD59-dependent manner

(**A-B**) Percentage cell death in JEG-3 NT control cells and JEG-3 hCD59 KO cells when exposed to increasing concentrations of the three TGY variants. Cells were incubated with toxins for 1.5 hours and cell death measured by an LDH-release cytotoxicity assay. Each point is the mean of 3 replicates, and error bars represent ±SD.

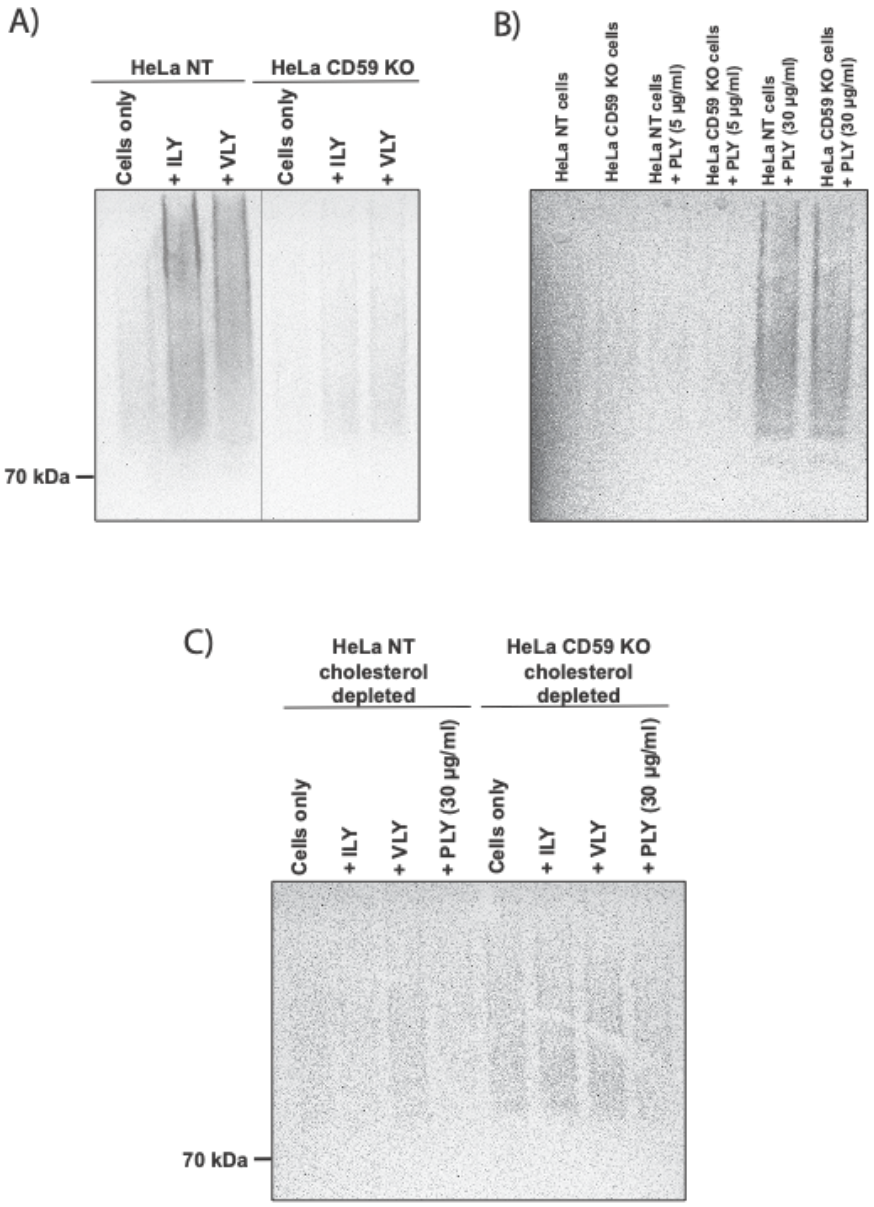

<u>Figure S3: Visualizing CDC oligomers for ILY, VLY and PLY on HeLa cells</u>

(**A-C**) Oligomerization of CDCs as assessed by SDS-AGE analysis. All CDCs were used at a concentration of 5 µg/ml, unless indicated otherwise. Cells were incubated with the indicated toxins on ice for 10 minutes before being prepared for western blotting. 0.01% glutaraldehyde was used as a cross-linker to preserve oligomers during sample preparation. Western blot membrane was probed with an anti-His-tag HRP-conjugated antibody.

	Primer name	Sequence (5'-3')
1.	PLY_D1-3_F	CTGGTGCCGCGCGGCAGCCATATGGCAAATAAAGCAGTAAATG
2.	PLY_D1-3_R_tgy	CGTTTTTATAAGCTGTAACCTTAGTCTC
3.	TGY_D4_F_ply	GGTTACAGCTTATAAAAACGGCTACCTG
4.	TGY_D4_R	AGTGGTGGTGGTGGTGGTGCTTAGTTGTTTTCAATTTCTTCG
5.	TGY_E454G_F	CACAAGGGTGGTTATGTGGCGC
6.	TGY_E454G_R	ATGCAGATTCAGGTAGCC
7.	TGY_E454A_F	CACAAGGGTGCATATGTGGCG
8.	TGY_E454A_R	ATGCAGATTCAGGTAGCC
9.	TGY_I544L_F	CGGCACCACCCTGCGCCCGAAAT
10.	TGY_I544L_R	TAGTTGGTGATGGTGCGTTTTTG
11.	T7_F	TAATACGACTCACTATAGGG
12.	T7_Term	GCTAGTTATTGCTCAGCGG

Table S1: Primers and oligonucleotides

Primers and oligonucleotides used for construction of hybrids (primers 1-4), site-directed mutagenesis (primers 5-10), and sequencing reactions (primers 11-12).